

Superparamagnetic Properties of Nanoparticles $\text{Ni}_{0.9}\text{Zn}_{0.1}\text{Fe}_2\text{O}_4$ for Biomedical Applications

Seung Wha Lee¹ and Chul Sung Kim^{2*}

¹Department of Electronic Engineering Chungju National University, Chungju 380-702, Korea

²Department of Physics, Kookmin University, Seoul 136-702, Korea

(Received 2 February 2005)

Nanoparticles $\text{Ni}_{0.9}\text{Zn}_{0.1}\text{Fe}_2\text{O}_4$ is fabricated by a sol-gel method. The magnetic and structural properties of powders were investigated with XRD, SEM, Mössbauer spectroscopy, and VSM. $\text{Ni}_{0.9}\text{Zn}_{0.1}\text{Fe}_2\text{O}_4$ powders annealed at 300 °C have a spinel structure and behaved superparamagnetically. The estimated size of $\text{Ni}_{0.9}\text{Zn}_{0.1}\text{Fe}_2\text{O}_4$ nanoparticle is about 10 nm. The hyperfine fields at 13 K for the A and B patterns are found to be 533 and 507 kOe, respectively. The ZFC curves are rounded at the blocking temperature (T_B) and show a paramagnetic-like behavior above T_B . T_B of $\text{Ni}_{0.9}\text{Zn}_{0.1}\text{Fe}_2\text{O}_4$ nanoparticle is about 250 K. Nanoparticles $\text{Ni}_{0.9}\text{Zn}_{0.1}\text{Fe}_2\text{O}_4$ annealed at 400 and 500 °C have a typical spinel structure and is ferrimagnetic in nature. The isomer shifts indicate that the iron ions were ferric at the tetrahedral (A) and the octahedral (B). The saturation magnetization of nanoparticles $\text{Ni}_{0.9}\text{Zn}_{0.1}\text{Fe}_2\text{O}_4$ annealed at 400 and 500 °C are 40 and 43 emu/g, respectively. The magnetic anisotropy constant of $\text{Ni}_{0.9}\text{Zn}_{0.1}\text{Fe}_2\text{O}_4$ annealed at 300 °C were calculated to be 1.6×10^6 ergs/cm³.

Key words : Superparamagnetism, Nanoparticle, Mössbauer, Applications in Biomedicine

1. Introduction

In recent years a lot of work has been done on nanocrystalline materials because of their unusual properties compared to the properties of bulk materials [1, 2]. In particular, superparamagnetic nanoparticles have been used in biomedicine and biotechnology as contrast agents in magnetic resonance imaging (MRI) and as drug carriers for magnetically guided drug delivery [3, 4]. Superparamagnetism has been extensively studied in the nanoparticles of pure metals such as Fe, Co, and Ni [5, 6]. However, these metal nanoparticles are chemically unstable. Thus, their applications are very limited. On the other hand, abundant and diverse magnetic metal oxides offer great opportunities for developing superparamagnetic nanoparticles with desirable properties. The nanoparticles of metal oxides such as spinel ferrites possess great potentials for applications since they are relatively inert and their magnetic properties can be fine tuned by chemical manipulations [7]. Solution routines are commonly used to fabricate ultrafine powders rather than

a solid-state reaction process. One of the solution routines is the sol-gel method, which is known as a technique for low temperature synthesis of glass, ceramic, and other materials. A few sol-gel methods for ultrafine cobalt, barium ferrite powders have been introduced [8, 9]. However, Zn-doped nanoparticles $\text{Ni}_{0.9}\text{Zn}_{0.1}\text{Fe}_2\text{O}_4$ has not yet been investigated to a great extent.

In this study, a sol-gel procedure was used for the preparation of nanoparticles $\text{Ni}_{0.9}\text{Zn}_{0.1}\text{Fe}_2\text{O}_4$ powders and their magnetic and structural properties as a function of annealing temperature were characterized by using an x-ray diffractometry, Mössbauer spectroscopy, and vibrating sample magnetometry (VSM) as well as scanning electron microscopy (SEM).

2. Experimental Procedures

Nanoparticles $\text{Ni}_{0.9}\text{Zn}_{0.1}\text{Fe}_2\text{O}_4$ was synthesized by a sol-gel method. The raw materials utilized in the present study were $\text{Ni}(\text{CH}_3\text{COO})_2 \cdot 4\text{H}_2\text{O}$, $\text{Zn}(\text{NO}_3)_2 \cdot 6\text{H}_2\text{O}$, and $\text{Fe}(\text{NO}_3)_3 \cdot 9\text{H}_2\text{O}$. These materials dissolved in ethylene glycol and distilled water for 30 min using an ultrasonic cleaner. The solution was refluxed at 80 °C for 12 h to allow the gel formation and then dried at 100 °C in a dry-

*Corresponding author: Tel: +82-2-910-4752,
Fax: +82-2-910-4728, e-mail: cskim@phys.kookmin.ac.kr

oven for 24 h. The dried powder was ground and annealed at temperatures ranging from 200 to 500 °C for 3 h in air. These compositions of samples annealed at various temperatures were identified by x-ray diffractometer with $\text{CuK}\alpha$ radiation. The mean particle size was calculated from the peak broadening in x-ray powder diffraction pattern by using Scherrer equation, and was confirmed by Scanning Electron Microscopy (JSM-6700F). The Mössbauer spectra were recorded using a conventional Mössbauer spectrometer of the electro-mechanical type with a 30 mCi ^{57}Co source in an Rh matrix [10]. Also, the saturation magnetization and coercivities of the powders were measured with a vibrating sample magnetometer (LakeShore 7300) at a maximum applied field of 15 kOe from 60 to 480 K.

3. Results and Discussion

X-ray diffraction patterns of $\text{Ni}_{0.9}\text{Zn}_{0.1}\text{Fe}_2\text{O}_4$ powders fired at various temperatures are shown in Fig. 1. The x-ray diffraction measurement shows that all peaks of $\text{Ni}_{0.9}\text{Zn}_{0.1}\text{Fe}_2\text{O}_4$ powders annealed at and above 300 °C are consistent with those of a standard pattern of a Ni-Zn ferrite [11]. In addition, the increase in the annealing temperature yields an increased sharpness of the major peak(311), that is, the growth of the larger grain size of $\text{Ni}_{0.9}\text{Zn}_{0.1}\text{Fe}_2\text{O}_4$ powders and improved crystallization. In Fig. 1, the formation of crystalline Ni-Zn ferrite is absorbed at and above 300 °C, however, the considerable broadening of all diffraction peaks of the sample fired at 300 °C suggests that the sizes of the Ni-Zn ferrite particles are relatively small.

The average particle sizes of all the heat-treated samples were determined from the line broadening of the (311) peaks using Scherrer method [12]. The average particle sizes of all the heat-treated samples are in the range 10 nm to 19 nm and are presented in Table 1. The SEM micrographs of the samples with $\text{Ni}_{0.9}\text{Zn}_{0.1}\text{Fe}_2\text{O}_4$ powders are shown in Fig. 2. The SEM micrographs indicate the distribution of grains uniform with really spherical shape. The value of the particle size of the

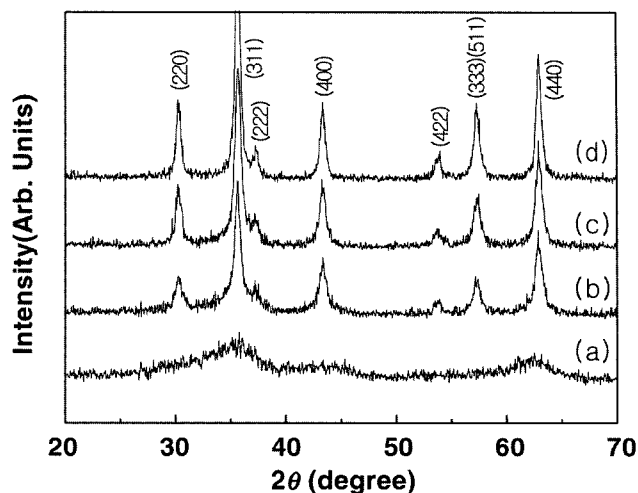


Fig. 1. X-ray diffraction patterns of $\text{Ni}_{0.9}\text{Zn}_{0.1}\text{Fe}_2\text{O}_4$ samples annealed at (a) 200 °C, (b) 300 °C, (c) 400 °C, (d) 500 °C.

samples was presented at Table 1, which shows that the particle size increases with increasing annealing temperature.

Mössbauer absorption spectra measured at room temperature and 14 K for $\text{Ni}_{0.9}\text{Zn}_{0.1}\text{Fe}_2\text{O}_4$ powders annealed at different temperatures are shown in Fig. 3 and Fig. 4, respectively. The room temperature Mössbauer spectrum (Fig. 3) of sample annealed at 200 °C show paramagnetic phase. Also, spectra of samples annealed, which were annealed at 400 and 500 °C, shows fitted with two six-line subpatterns that are assigned to A-ions in tetrahedral sites and B-ions in octahedral sites of a typical cubic spinel ferrite.

However, the Mössbauer spectrum (Fig. 4) for the samples annealed at 300 °C exhibit a quadrupole splitting component at the center of the spectrum and a magnetically split component spread across the spectrum. The presence of both quadrupole and magnetic splitting is due to the existence of a size distribution in the nanocomposite. This observation is similar to what was reported by Ahmed *et al.* [13]. At room temperature, the quadrupole splitting dominates the magnetic splitting, and hence the sample becomes superparamagnetic. The inten-

Table 1. Analyzed results of Mössbauer spectra for $\text{Ni}_{0.9}\text{Zn}_{0.1}\text{Fe}_2\text{O}_4$ nanoparticles

annealed temp. (°C)	measured temp. (K)	average particle size (nm)	fitted spectrum	hyperfine field (kOe)		quadruple splitting (mm/s)		isomer shift (mm/s)	
				B	A	B	A	B	A
300	13		sextet	533	507	0.00	0.00	0.36	0.28
300	300	10	sextet	471	424	0.00	0.00	0.19	0.16
			doublet	–	–		0.51		0.10
400	300	16	sextet	475	442	0.00	0.00	0.17	0.14
500	300	19	sextet	486	453	0.00	0.00	0.18	0.15

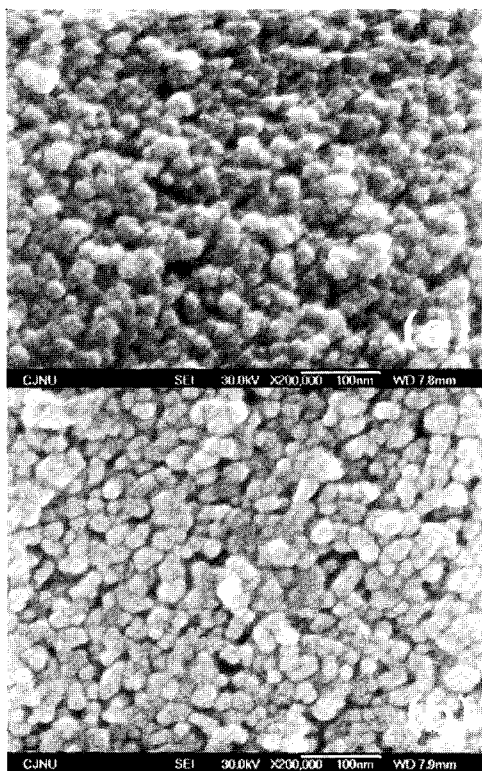


Fig. 2. SEM micrographs of $\text{Ni}_{0.9}\text{Zn}_{0.1}\text{Fe}_2\text{O}_4$ samples annealed at (a) 300°C, (b) 500°C.

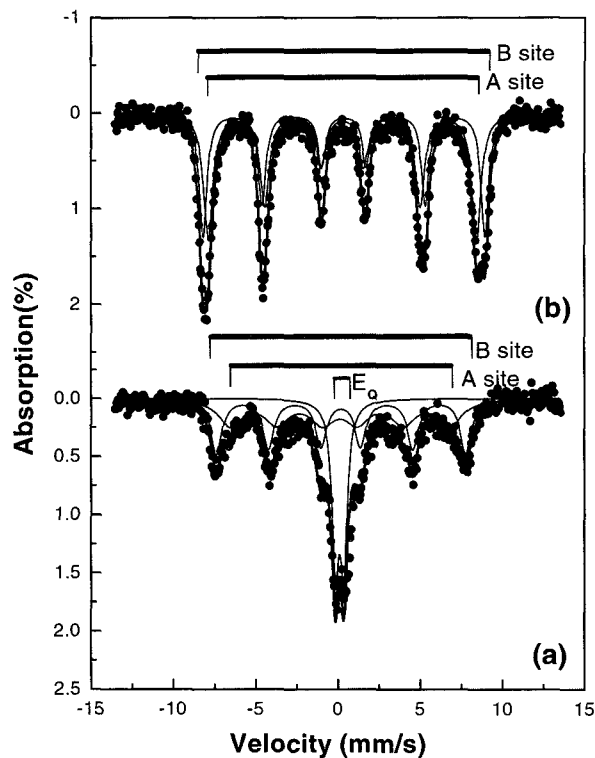


Fig. 4. The Mössbauer spectra of $\text{Ni}_{0.9}\text{Zn}_{0.1}\text{Fe}_2\text{O}_4$ annealed at 300°C measured at (a) 300 K, (b) 13 K.

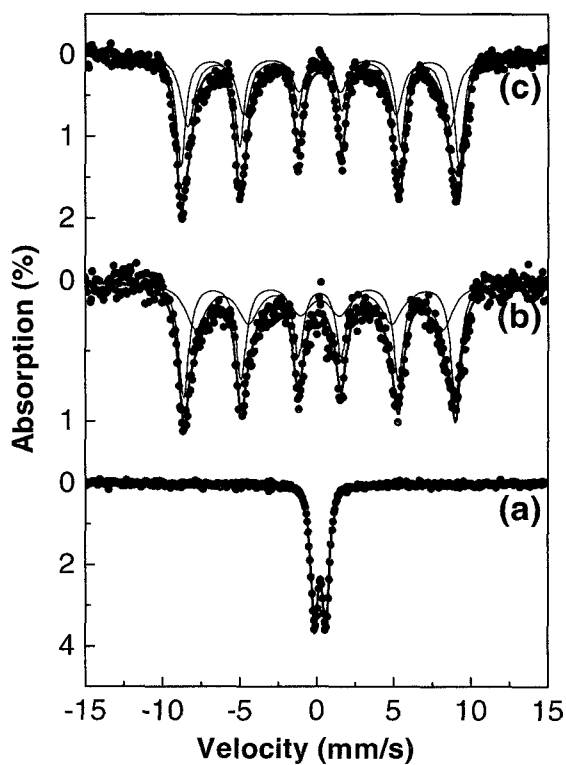


Fig. 3. Room temperature Mössbauer spectra of $\text{Ni}_{0.9}\text{Zn}_{0.1}\text{Fe}_2\text{O}_4$ samples annealed at (a) 200°C, (b) 400°C, (c) 500°C.

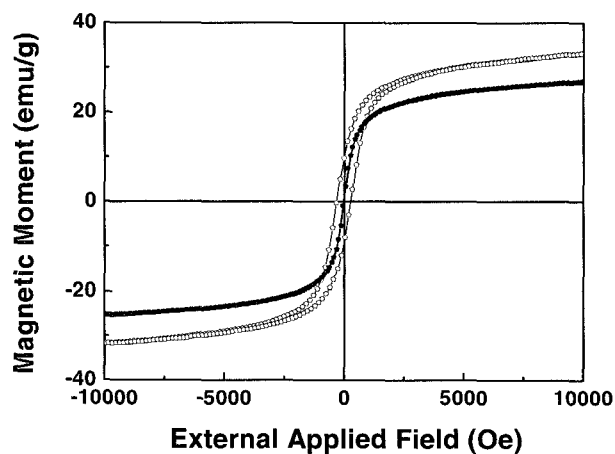


Fig. 5. (a) Magnetization vs applied magnetic field curve of the $\text{Ni}_{0.9}\text{Zn}_{0.1}\text{Fe}_2\text{O}_4$ annealed at 300°C. The solid and dotted lines have measured at 60 and 300 K.

sity of quadrupole splitting decreases with temperature. At 14 K, only the magnetic splitting is present and the $\text{Ni}_{0.9}\text{Zn}_{0.1}\text{Fe}_2\text{O}_4$ powder is completely ferrimagnetic. Table 1 gives the Mössbauer parameters obtained from least square fits of the spectra [14]. The isomer shifts at room temperature for the A and B patterns were found to be (0.14~0.16) and (0.17~0.19) mm/s relative to the Fe

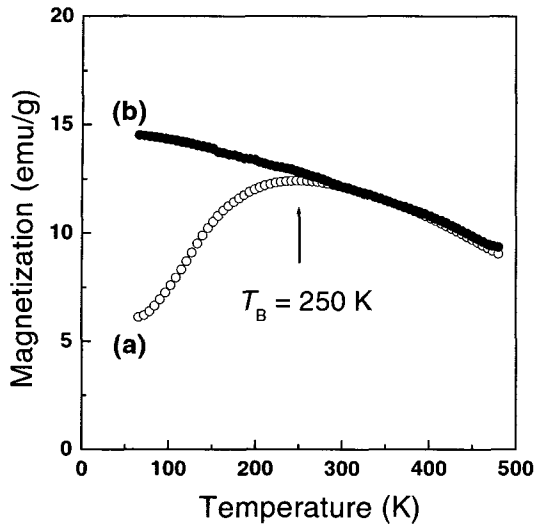


Fig. 6. The magnetization vs temperature of $\text{Ni}_{0.9}\text{Zn}_{0.1}\text{Fe}_2\text{O}_4$ annealed at 300°C represent measured under a 200 Oe field with ZFC and FC process.

metal, respectively, which are consistent with high-spin Fe^{3+} charge states [15].

Magnetic properties of the superparamagnetic nanoparticle $\text{Ni}_{0.9}\text{Zn}_{0.1}\text{Fe}_2\text{O}_4$ annealed at 300°C were investigated with VSM from 60 to 300 K. Figure 5 shows the magnetization versus magnetic field curves of the sample annealed at 300°C , measured at 60 K (solid line) and 300 K (dotted line). At low temperatures, the sample annealed at 300°C , exhibits a hysteretic behavior, indicating that it has ferrimagnetic phase. However, at room temperature, the ferrimagnetic hysteresis seems to have disappeared. Figure 5 shows the temperature dependence of the magnetization of the Ni-Zn ferrite annealed at 300°C . Also, according to the Stoner-Wohlfarth theory [16], the coercivity H_C of a single-domain particle is the following: $H_C = 2K/\mu_0 M_S$, where μ_0 is a universal constant of permeability in free space and M_S is the saturation magnetization of the nanoparticle. Above the blocking temperature, the magneto crystalline anisotropy is overcome by thermal activation, and K can be considered as zero. The nanoparticles do not display any magnetization hysteresis behavior with $H_C = 0$.

As a typical blocking behavior of superparamagnetic nanoparticles, the $\text{Ni}_{0.9}\text{Zn}_{0.1}\text{Fe}_2\text{O}_4$ nanoparticles show a different magnetization process when the sample is cooled below the blocking temperature with an external magnetic field. Plot (b) in Fig. 6 shows the magnetization of the sample that is field cooled (FC) from 480 to 60 K under an applied field of 200 Oe. The FC magnetization shows its maximum at 60 K, and it decreases steadily with increasing temperature. After the temperature rises

above the blocking temperature, this plot overlaps with the one obtained from zero-field cooled (ZFC) process (plot (a) in Fig. 6). For $\text{Ni}_{0.9}\text{Zn}_{0.1}\text{Fe}_2\text{O}_4$ nanoparticles with a size of 10 nm, the blocking temperature appears at 250 K when an external field of 200 Oe applied.

The magnetic anisotropy constant (K) was deduced from the blocking temperature using the equation $K = 25k_B T_B/V$, where k_B is the Boltzman constant and V is the volume of particle [6]. The magnetic anisotropy constant of $\text{Ni}_{0.9}\text{Zn}_{0.1}\text{Fe}_2\text{O}_4$ annealed at 300°C were calculated to be 1.6×10^6 ergs/cm³. For biomedicine application, such as hyperthermia, drug delivery system (DDS), and so on, magnetic fluid carrier should not lump for the smooth circulation of the blood and should not be sharp for the prevention of a hurt. Therefore, they should be superparamagnetic and have the spherical shape. It is considered that $\text{Ni}_{0.9}\text{Zn}_{0.1}\text{Fe}_2\text{O}_4$ annealed at 300°C , are available for biomedical applications such as hyperthermia and drug delivery system as a magnetic fluid carrier because it has spherical shape, narrow particle distribution, chemical stability, and superparamagnetic behavior.

4. Conclusion

$\text{Ni}_{0.9}\text{Zn}_{0.1}\text{Fe}_2\text{O}_4$ nanoparticles with different diameters have been prepared and their structural and magnetic properties have been investigated by XRD, VSM, SEM, and Mössbauer spectroscopy. $\text{Ni}_{0.9}\text{Zn}_{0.1}\text{Fe}_2\text{O}_4$ powder annealed at 300°C has spinel structure and behaved superparamagnetically. The estimated size of superparamagnetic $\text{Ni}_{0.9}\text{Zn}_{0.1}\text{Fe}_2\text{O}_4$ nanoparticle is about 10 nm. The hyperfine fields at 13 K for the A and B patterns were found to be 533 and 507 kOe, respectively. The blocking temperature (T_B) of superparamagnetic $\text{Ni}_{0.9}\text{Zn}_{0.1}\text{Fe}_2\text{O}_4$ nanoparticle is about 250 K. The magnetic anisotropy constant of $\text{Ni}_{0.9}\text{Zn}_{0.1}\text{Fe}_2\text{O}_4$ annealed at 300°C was calculated to be 1.6×10^6 ergs/cm³. It is considered that $\text{Ni}_{0.9}\text{Zn}_{0.1}\text{Fe}_2\text{O}_4$ powder annealed at 300°C is available for biomedicine application such as hyperthermia and drug delivery system as a magnetic fluid carrier.

Acknowledgments

This research was sponsored by the Korea Science and Engineering Foundation through the Research Center for Advanced Magnetic Materials at Chungnam National University.

References

- [1] Adam J. Rondinone, Anna C. S. Samia, and Z. J. Zhang,

- Appl. Phys. Lett., **76**(24), 3624 (2000).
- [2] S. W. Lee, K. W. Woo, C. S. Kim, J. of Magnetism **9**(3), 83 (2004).
- [3] Perdo Tartaj, Maria del Puerto Morales, Sabino Veintemillas-Veraguer and Carlos J Serna. J. Phys. D: Appl. Phys., **36** R182 (2003).
- [4] S. H. Im, T. Herricks, Y. T. Lee, Y. Xia, Chem. Phys. Lett., **401**, 19 (2005).
- [5] S. K. Khanna and S. Linderth, Phys. Rev. Lett. **67**, 742 (1991).
- [6] Qi Chen and Z. J. Zhang, Appl. Phys. Lett. **73**, 3156 (1998).
- [7] S. W. Lee, Y. G. Ryu, K. J. Yang, K. D. Jung, S. Y. An, and C. S. Kim, J. Appl. Phys., **91**(10), 610 (2002).
- [8] J. G. Lee, H. M. Lee, C. S. Kim, and Y. J. Oh, J. Magn. Mater. **177-181**, 900 (1998).
- [9] V. K. Sankaranarayana, Q. A. Pankhurst, D. P. Dickson, and C. E. Johnson, J. Magn. Mater. **125**, 199 (1998).
- [10] S. J. Kim, K. D. Jung, and C. S. Kim, Hyperfine Interactions **156**, 113 (2004).
- [11] C. Caizer, Mater. Science and Eng. B **100**, 63 (2003).
- [12] B. K. Nath, P. K. Chakrabarti, S. Das, U. Kumar, P. K. Mukhopadhyay, and D. Das, Eur. Phys. B **39**, 417 (2004).
- [13] Sufi R. Ahmed, S. B. Ogale, Georgia C. Papaefthymiou, Ramamoorthy Ramesh, and Peter Kofinas, Appl. Phys. Lett. **80**(9), 1616 (2002).
- [14] S. W. Lee, S.Y. Yoon, S. Y. An, W. C. Kim, and C. S. Kim, J. of Magnetism **4**(4), 115 (1999).
- [15] H. N. Ok, K. S. Baek, H. S. Lee, and C. S. Kim, Phys. Rev. B **41**, 62 (1990).
- [16] S. Chikazumi, *Physics of Ferromagnetism*, 2nd ed. (Oxford University Press, New York, 1997), p. 510.